

LETTERS

A single-molecule optical transistor

J. Hwang¹, M. Pototschnig¹, R. Lettow¹, G. Zumofen¹, A. Renn¹, S. Götzinger¹ & V. Sandoghdar¹

The transistor is one of the most influential inventions of modern times and is ubiquitous in present-day technologies. In the continuing development of increasingly powerful computers as well as alternative technologies based on the prospects of quantum information processing, switching and amplification functionalities are being sought in ultrasmall objects, such as nanotubes, molecules or atoms^{1–9}. Among the possible choices of signal carriers, photons are particularly attractive because of their robustness against decoherence, but their control at the nanometre scale poses a significant challenge as conventional nonlinear materials become ineffective. To remedy this shortcoming, resonances in optical emitters can be exploited, and atomic ensembles have been successfully used to mediate weak light beams⁷. However, single-emitter manipulation of photonic signals has remained elusive and has only been studied in high-finesse microcavities^{10–13} or waveguides^{8,14}. Here we demonstrate that a single dye molecule can operate as an optical transistor and coherently attenuate or amplify a tightly focused laser beam, depending on the power of a second ‘gating’ beam that controls the degree of population inversion. Such a quantum optical transistor has also the potential for manipulating non-classical light fields down to the single-photon level. We discuss some of the hurdles along the road towards practical implementations, and their possible solutions.

The central phenomenon behind the operation of a transistor is nonlinearity. A simple two-level atom is known to undergo nonlinear interaction with light¹⁵, but it is usually not considered as a sufficiently strong medium for manipulating laser beams in free space. In a recent theoretical study, however, we showed that in the weak excitation regime, an atom can block a propagating light beam fully if it is in a directional dipolar mode, and by up to 85% if it is a tightly focused plane wave¹⁶. In these cases, photons are confined to an area comparable with the scattering cross-section of the atom, and their electric fields become large enough to achieve atomic excitation with unity or near unity probability. As we shall see below, this strong coupling between an emitter and light also makes it possible to observe stimulated emission from a single molecule, and paves the way for the realization of various nonlinear phenomena at the single-emitter level.

The emitters of choice in our study are dye molecules embedded in organic crystalline matrices. These are highly suitable for quantum optical investigations because under cryogenic conditions, the zero-phonon lines (ZPLs) connecting the vibronic ground states of their electronic ground ($|1\rangle$) and excited ($|2\rangle$) states become lifetime limited¹⁷ (Fig. 1a). If the doping concentration is low enough, single dye molecules can be selectively addressed spectrally¹⁸. The most common way of achieving this is through fluorescence excitation spectroscopy, where the frequency of a narrow-band laser is scanned across the inhomogeneous distribution of the ZPLs¹⁹, and the Stokes-shifted fluorescence to the vibronic excited states ($|4\rangle$) in Fig. 1a) of the electronic ground state is recorded. In addition, it has been demonstrated that single molecules can be detected resonantly by

the interference of a laser beam with its coherent scattering²⁰. Recently, the latter technique was extended to show that a molecule can attenuate a strongly confined laser beam by about 10%, both in the near and far fields^{21,22}. The degree of this attenuation has been found to be smaller than its theoretical limit for a two-level atom¹⁶, mainly because the Stokes-shifted fluorescence acts as a loss channel and reduces the coherent scattering cross-section of the ZPL^{21,22}. Another

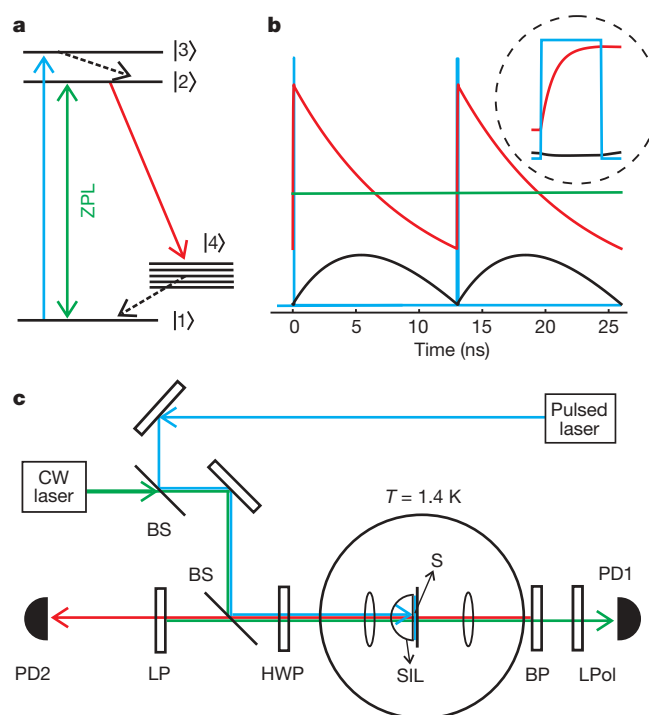


Figure 1 | Diagrams of the experiment. **a**, Energy level scheme of a molecule with ground state ($|1\rangle$), and ground ($|2\rangle$) and first excited ($|3\rangle$) vibrational states of the first electronic excited state. Manifold $|4\rangle$ shows the vibronic levels of the electronic ground state, which decay rapidly to $|1\rangle$. Blue arrow, excitation by the gate beam; green double-headed arrow, coherent interaction of the CW source beam with the zero-phonon line (ZPL); red arrow, Stokes-shifted fluorescence; black dashed arrows, non-radiative internal conversion. **b**, Time-domain description of laser excitations and corresponding response of the molecule simulated by the Bloch equations with periodic boundary conditions. Blue spikes and red curve represent the pump laser pulses and the population of the excited state $|2\rangle$, respectively. Black curve shows the time trajectory of $\text{Im}(\rho_{21})$. Straight green line indicates the constant probe laser intensity that is on at all times. Inset, magnified view of curves during a laser pulse. **c**, Schematic diagram of the optical set-up. BS, beam splitter; LP, long-pass filter; BP, band-pass filter; HWP, half-wave plate; LPol, linear polarizer; S, sample; SIL, solid-immersion lens; PD1, PD2, avalanche photodiodes. Transmission of the probe beam (green) is monitored on PD1, and the Stokes-shifted fluorescence (red) is recorded on PD2.

¹Laboratory of Physical Chemistry and optETH, ETH Zurich, 8093 Zurich, Switzerland.

source of decoherence is the weak coupling of the dye molecule to the host matrix. These two effects can vary in different systems, and amount roughly to a 2–5 times reduction of the scattering cross-section.

The first step in our experiment was to detect single dibenzanthanthrene (DBATT) molecules doped in a *n*-tetradecane matrix. To do this, we used a continuous-wave (CW) ring dye laser (wavelength ~ 590 nm, linewidth ~ 1 MHz) to perform fluorescence excitation and extinction spectroscopy on the $|1\rangle \leftrightarrow |2\rangle$ ZPL transitions. Once a molecule was selected, we used a synchronously pumped pulsed dye laser (wavelength ~ 582 nm, pulse width $t_{\text{pul}} \approx 50$ ps, repetition period $t_{\text{rep}} = 13$ ns) to populate the vibronic excited state of its first electronic excited state ($|3\rangle$ in Fig. 1a). The $|1\rangle \leftrightarrow |3\rangle$ transition has a broad linewidth of about 30 GHz (ref. 23), determined by the fast vibrational relaxation of $|3\rangle$ to $|2\rangle$. State $|2\rangle$, on the other hand, has a relatively long fluorescence lifetime of 9.5 ns (ref. 24) so that population inversion in this state could be achieved right after each pulse. Figure 1b gives a pictorial temporal view of the excitation and emission processes. As we shall see below, the pulsed and the CW laser beams served as the transistor gate and source, respectively. The experimental arrangement of the single-molecule microscope operating at $T = 1.4$ K, as well as the excitation and detection paths, are sketched in Fig. 1c and are described in more detail in ref. 22. Here we emphasize that in order to provide a high coupling efficiency to the molecule, both laser beams were strongly focused to near the diffraction limit.

The data points in Fig. 2a–e display a series of transmission spectra recorded on a weak CW laser beam for various powers of the pulsed laser beam. Figure 2a shows that in the absence of the pump beam, the molecule attenuates the source beam by about 7%. However, as the gate power is raised and the population is transferred from the ground to the excited state, the dip decreases, until the $|1\rangle \rightarrow |2\rangle$ transfer rate equalizes the spontaneous decay rate of $|2\rangle$ and the molecule becomes fully transparent to the probe beam (Fig. 2c). If the pump power is increased even further, population inversion is achieved and we observe amplification of the probe laser beam (Fig. 2d and e). These data demonstrate that a single molecule can indeed act as a transistor, in which the pulsed gate beam regulates the flow of the CW source beam by controlling the populations of the molecular ground and excited states. The data points in Fig. 2f summarize the transistor characteristic curve by plotting the visibility (the ratio of the peak or dip magnitude to the off-resonance signal) for the transmission of the source as a function of the gate power.

The underlying mechanism of light amplification by a population-inverted molecule is analogous to its extinction by a ground-state molecule. The dip in Fig. 2a arises from the destructive interference between the excitation laser beam and the light that is coherently scattered by the molecule^{21,22}, causing the reflection of the incident beam¹⁶. Similarly, amplification by stimulated emission can be understood as a constructive interference of the two fields when the molecule is in the excited state. To elucidate the coherent nature of light amplification experimentally, we allowed a slight polarization ellipticity for the source beam and placed a polarizer to select a projection of the molecular and laser fields with a relative phase of 90° (more details may be found in ref. 22). Figure 3a shows the resulting dispersive transmission spectrum in the absence of pumping. When a strong gate beam was turned on, the spectrum was

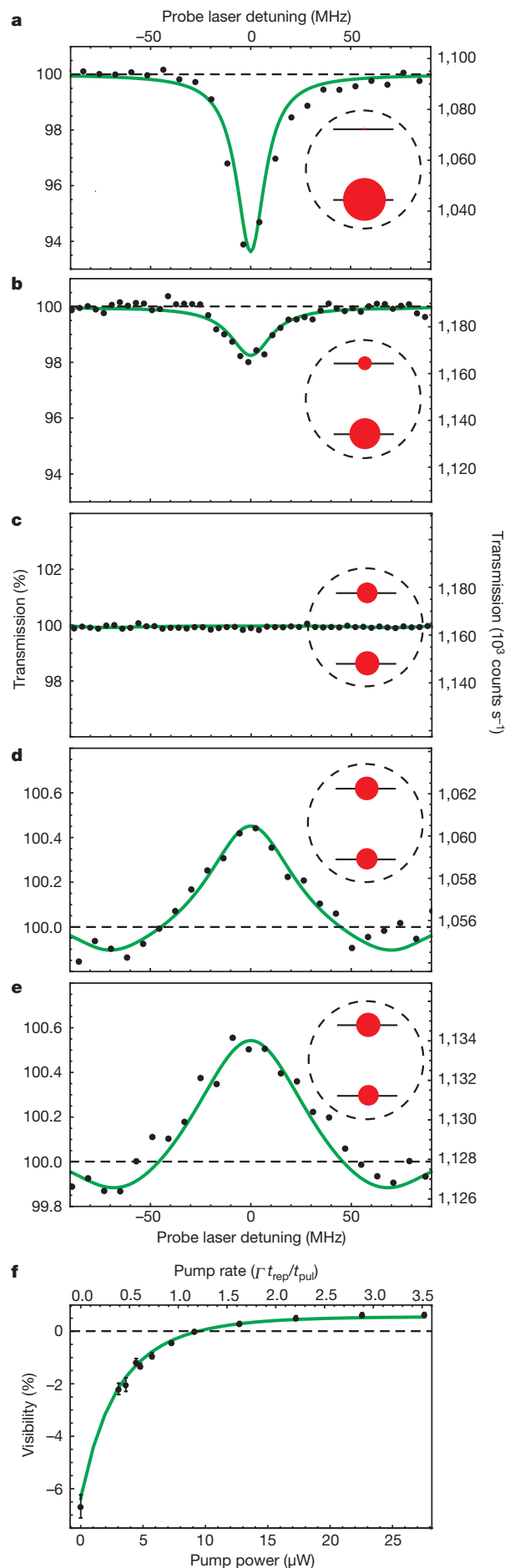


Figure 2 | Attenuation and amplification of a laser beam by a single molecule. **a–e**, Filled circles, transmission of a weak CW laser beam as a function of its frequency detuning with respect to the ZPL of a single dye molecule. Average pump laser powers (μW) were: 0 (**a**), 3.6 (**b**), 9.1 (**c**), 17.3 (**d**) and 27.6 (**e**). Insets indicate the time-averaged populations of states $|1\rangle$ and $|2\rangle$. The radii of the circles are proportional to the populations. **f**, Filled circles, visibility of the transmission spectra with respect to the pump power. Solid curves in all panels are outcomes of calculations (see text for details). Error bars in **f** were determined by propagating errors based on the 95% confidence intervals of the amplitude and background in Lorentzian fits to the experimental spectra.

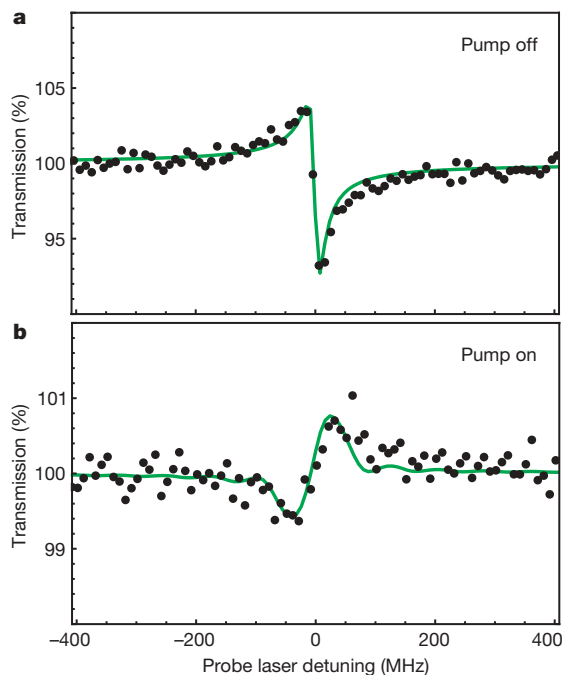


Figure 3 | Coherent scattering phase shift of π on population inversion. **a**, Filled circles, transmission spectrum of the probe beam for a single molecule in the ground state (pump off). By adjusting the polarization state of the incident light and an analyser in detection, the phase between the laser beam and the light scattered by the molecule could be adjusted to obtain a dispersive spectrum. **b**, Same measurement as in **a** but on a population-inverted molecule (pump on) yields a dispersive spectrum with 180° (π) phase shift. Solid curves are outcomes of calculations; see text for details.

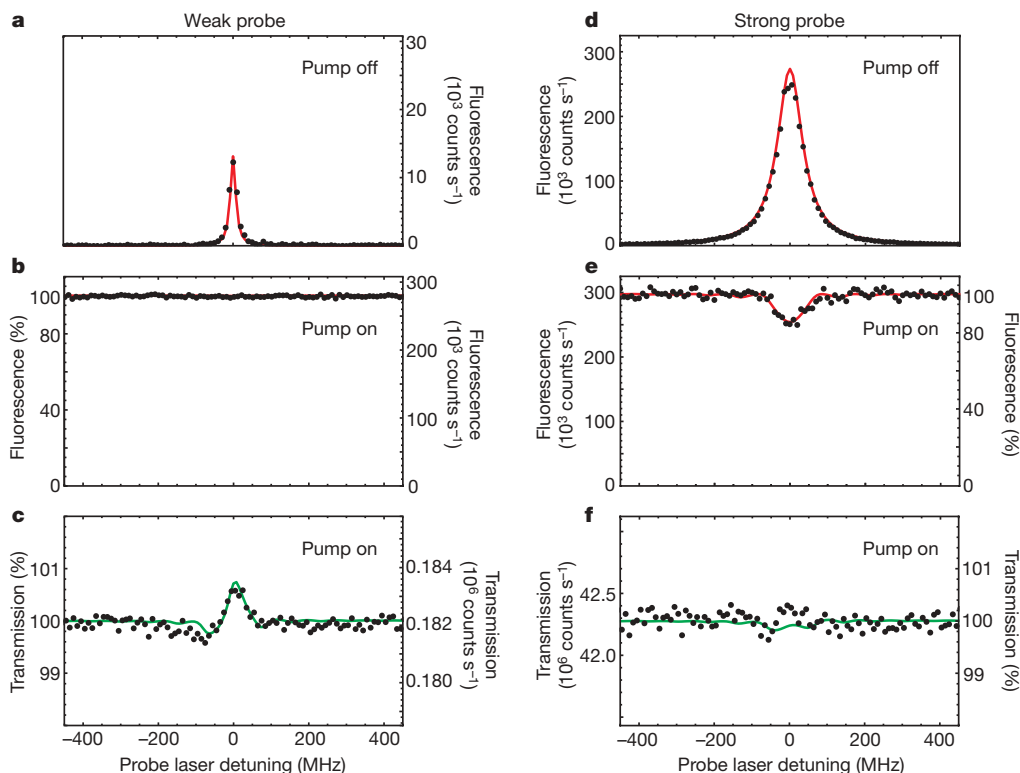


Figure 4 | The nonlinear response of a population-inverted molecule. Filled circles, spectra recorded with the CW laser power corresponding to saturation parameter $S = 0.05$ (left column) and $S = 22.3$ (right column). **a, d**, Fluorescence excitation spectra in the absence of pumping. In **a**, a natural linewidth of 17 MHz verifies that the Rabi frequency Ω is much smaller than the spontaneous decay rate Γ . **b, e**, Fluorescence of state $|2\rangle$ caused by a strong pump beam as a function of the CW laser frequency. In

modified to that displayed in Fig. 3b, revealing a π phase shift in the light scattered by the excited-state molecule. Hence, the single-emitter transistor has two output channels—one in transmission and one in reflection¹⁶—which are fed depending on whether the emitter is prepared in the excited or ground state, respectively.

Having established the coherent character of the amplification process, it is evident that a single-emitter transistor operates efficiently only in the unsaturated regime^{15,22}. We, thus, elaborate on the performance of this device as a function of the source power. A strong pump beam populates state $|2\rangle$ every 13 ns, comparable with the fluorescence lifetime of 9.5 ns (Fig. 1b). Therefore, if the probe beam power is kept well below the saturation level, the stimulated emission of state $|2\rangle$ is much weaker than its spontaneous emission¹⁵, so that a substantial Stokes-shifted fluorescence is registered on PD2 (see Fig. 1c). Figure 4a–c illustrates that under these conditions, tuning the frequency of the probe laser to the molecular ZPL does not lead to a notable depletion of population in $|2\rangle$, but it does cause a sizable amplification. The situation was very different when the probe beam was strong enough to power broaden the $|1\rangle \leftrightarrow |2\rangle$ transition, as represented by the fluorescence excitation spectrum in Fig. 4d. The data points in Fig. 4e and f show that now, the population of state $|2\rangle$ is clearly depleted by the probe laser, but the amplification of this beam is not significant. In this saturated regime (see equation (2) below), stimulated emission on the ZPL constitutes a very small part of the strong transmitted power and cannot be deciphered on its noisy base line. The depletion of fluorescence from level $|2\rangle$, on the other hand, becomes observable because it is a considerable fraction of the fixed total fluorescence, which is set by the pumping rate. Thus, we point out that although both laser-induced depletion of the excited state population²⁵ and light amplification¹⁵ are associated with stimulated emission, to observe the former it is sufficient to apply a high laser power, while direct detection of the latter has been

e, a strong probe laser depletes the population of $|2\rangle$. **c, f**, Transmission spectra recorded simultaneously with the data in **b** and **e**, respectively. A weak probe laser beam is amplified by a population-inverted molecule (**c**) but the effect of the molecule is negligible on a strong probe beam (**f**). All vertical axes present a quantitative account of the experimental detector signals. Solid curves are outcomes of calculations; see text for details.

made possible here only because of a strong coupling between the laser beam and the emitter.

The interaction of a multilevel molecule with classical light can be analysed using the formalism of the optical Bloch equations^{22,24}. Given the fast incoherent decays of $|3\rangle$ to $|2\rangle$ and $|4\rangle$ to $|1\rangle$, however, these decays and the pumping transition $|1\rangle \rightarrow |3\rangle$ can be expressed by rates, simplifying the problem to the coherent treatment of a two-level system. The imaginary part of the resulting off-diagonal density matrix element ρ_{21} is directly proportional to the electric field of the coherently scattered light on the ZPL resonance¹⁵, thus allowing us to calculate the power associated with its interference with the excitation field^{16,21,22}. Furthermore, the diagonal element ρ_{22} is proportional to the total power dissipated out of the excited state. To consider the case of pulsed population inversion, we applied periodic boundary conditions on the elements of ρ . The time dependence of ρ_{21} and ρ_{22} are depicted respectively by the black and red curves in Fig. 1b, and the inset shows the evolution of these quantities during the pulse. The solid curves in Figs 2, 3 and 4 display the outcome of our numerical calculations for pulsed excitation, which show excellent agreement with the experimentally obtained data. The high quantitative success of the fits in Figs 4a–c and 4d–f are particularly noteworthy, because each set of spectra was fitted simultaneously, sharing the values of the pump power, probe power, and collection efficiency where applicable.

It is instructive to present the steady-state solutions of ρ for the case of CW pumping, which can be formulated analytically as:

$$\rho_{22}^{\text{ss}} = \frac{\xi}{1+\xi} + \frac{1-\xi}{1+\xi} \frac{\Omega^2}{4\Delta^2 + (1+\xi)^2\Gamma^2 + 2\Omega^2} \quad (1)$$

$$\rho_{21}^{\text{ss}} = \frac{1-\xi}{1+\xi} \frac{\Omega[2\Delta - i\Gamma(1+\xi)]}{4\Delta^2 + (1+\xi)^2\Gamma^2 + 2\Omega^2} \quad (2)$$

Here the ratio $\xi = k/\Gamma$ provides a measure for the pumping strength, where k is the $|1\rangle \rightarrow |2\rangle$ pumping rate, Δ represents the frequency detuning between the probe laser and the ZPL, Ω is the Rabi frequency, and Γ denotes the spontaneous emission rate. The first term of ρ_{22}^{ss} yields the population of $|2\rangle$ due to pumping alone, that is, for $\Omega = 0$. One clearly sees that the second term of ρ_{22}^{ss} and ρ_{21}^{ss} change sign when ξ crosses the value of 1. The fraction of light removed or added to the transmitted probe laser beam on resonance and in the weak excitation regime turns out to be expressed by $R \propto (1-\xi)/(1+\xi)^2$, which assumes positive and negative values for attenuation and amplification, respectively. It follows that R becomes zero at $\xi = 1$ and takes on its minimum value (that is, maximum amplification) at $\xi = 3$. These results can be qualitatively extended to the case of pulsed population inversion if ξ is replaced by $\xi = kt_{\text{pul}}/(t_{\text{rep}}\Gamma)$, where t_{pul} and t_{rep} are the pulse on-time and repetition period, respectively. More quantitatively, for the parameters of our experiment, the crossover between attenuation and amplification takes place at $\xi \approx 1.2$, and the maximum value of amplification is reached at $\xi \approx 6$ for pulsed pumping. We remark in passing that the single-molecule transistor can also operate using a CW gate beam.

The analytical results for CW pumping also provide us with intuitive insight into the spectral features of the data in Fig. 2. First, we note that the linewidth of the amplified spectrum in Fig. 2e is more than twice as broad as the extinction spectrum recorded on the ground state in Fig. 2a. This is caused by the strong pumping rate k , which is necessary for counter-balancing spontaneous emission and achieving population inversion. A large k is also responsible for the reduction of the visibility from 7% for the extinction dip to 0.6% for the amplification peak because it provides a loss channel for the ground state and lowers the scattering cross-section of the $|1\rangle \leftrightarrow |2\rangle$ transition. The optimum ratio between amplification and extinction is found to be $-1/8$ at $\xi = 3$ for CW pumping, determined by the ratios of the minimum and maximum of R . Finally, we note

that the weak modulations observed at ± 76 MHz in Figs 2d, e, and 4c, f result from the periodic pump process.

The operation realm of single-emitter quantum optical transistors can be extended in several ways. We have shown that such a device can control a source beam that has a weaker flux than its saturated emission rate. To push the power range of the source to higher values, one could enhance the excited-state spontaneous emission rate by coupling to nano-antennas^{26,27} or simple microcavity geometries²⁸. This would also diminish the impact of Stokes-shifted fluorescence, which reduces the coherent scattering cross-section of dye molecules. At the other extreme, because the geometric coupling of a light beam to a single emitter can reach unity^{16,29}, it is expected that single-emitter transistors can also manipulate non-classical source beams with only a few photons. Indeed, preliminary experiments have demonstrated 10% attenuation of a light beam with as few as about 1,000 photons per second²². In addition, the gate power can be reduced to only a few tens of photons per pulse if the molecular population is inverted in a resonant pumping scheme through the narrow ZPL³⁰, instead of the broad $|1\rangle \leftrightarrow |3\rangle$ transition. Such a coherent pumping could also prepare superpositions of states $|1\rangle$ and $|2\rangle$, which would be then stamped onto photons scattered in the forward and backward directions. Given that a molecule only occupies a few nanometres in the solid state, it should be possible to package a huge number of single-emitter transistors in a nanoscopic area and exploit the inhomogeneous distribution of frequencies to operate many signals simultaneously.

Received 19 March; accepted 14 May 2009.

1. Tans, S. J., Verschuereen, A. R. M. & Dekker, C. Room-temperature transistor based on a single carbon nanotube. *Nature* **393**, 49–52 (1998).
2. Park, J. *et al.* Coulomb blockade and the Kondo effect in single-atom transistors. *Nature* **417**, 722–725 (2002).
3. Liang, W., Shores, M. P., Bockrath, M., Long, J. R. & Park, H. Kondo resonance in a single-molecule transistor. *Nature* **417**, 725–729 (2002).
4. Davidovich, L., Maali, A., Brune, M., Raimond, J. M. & Haroche, S. Quantum switches and nonlocal microwave fields. *Phys. Rev. Lett.* **71**, 2360–2363 (1993).
5. Harris, S. E. & Yamamoto, Y. Photon switching by quantum interference. *Phys. Rev. Lett.* **81**, 3611–3614 (1998).
6. Micheli, A., Daley, A. J., Jaksch, D. & Zoller, P. Single atom transistor in a 1d optical lattice. *Phys. Rev. Lett.* **93**, 140408 (2004).
7. Dawes, A. M. C., Illing, L., Clark, S. M. & Gauthier, D. J. All-optical switching in rubidium vapor. *Science* **308**, 672–674 (2005).
8. Chang, D. E., Sorensen, A. S., Demler, E. A. & Lukin, M. D. A single-photon transistor using nanoscale surface plasmons. *Nature Phys.* **3**, 807–812 (2007).
9. Vaishnav, J., Ruseckas, J., Clark, C. W. & Juzelunas, G. Spin field effect transistors with ultracold atoms. *Phys. Rev. Lett.* **101**, 265302 (2008).
10. Imamoglu, A., Schmidt, H., Woods, G. & Deutsch, M. Strongly interacting photons in a nonlinear cavity. *Phys. Rev. Lett.* **79**, 1467–1470 (1997).
11. Duan, L.-M. & Kimble, H. J. Scalable photonic quantum computation through cavity-assisted interactions. *Phys. Rev. Lett.* **92**, 127902 (2004).
12. Birnbaum, K. M. *et al.* Photon blockade in an optical cavity with one trapped atom. *Nature* **436**, 87–90 (2005).
13. Schuster, I. *et al.* Nonlinear spectroscopy of photons bound to one atom. *Nature Phys.* **4**, 382–385 (2008).
14. Shen, J.-T. & Fan, S. Strongly correlated two-photon transport in a one-dimensional waveguide coupled to a two-level system. *Phys. Rev. Lett.* **98**, 153003 (2007).
15. Loudon, R. *Quantum Theory of Light* (Oxford Univ. Press, 2000).
16. Zumofen, G., Mojarad, N. M., Sandoghdar, V. & Agio, M. Perfect reflection of light by an oscillating dipole. *Phys. Rev. Lett.* **101**, 180404 (2008).
17. Moerner, W. E. & Orrit, M. Illuminating single molecules in condensed matter. *Science* **283**, 1670–1676 (1999).
18. Moerner, W. E. & Kador, L. Optical detection and spectroscopy of single molecules in a solid. *Phys. Rev. Lett.* **62**, 2535–2538 (1989).
19. Orrit, M. & Bernard, J. Single pentacene molecules detected by fluorescence excitation in a *p*-terphenyl crystal. *Phys. Rev. Lett.* **65**, 2716–2719 (1990).
20. Plakhotnik, T. & Palm, V. Interferometric signatures of single molecules. *Phys. Rev. Lett.* **87**, 183602 (2001).
21. Gerhardt, I. *et al.* Strong extinction of a laser beam by a single molecule. *Phys. Rev. Lett.* **98**, 033601 (2007).
22. Wrigge, G., Gerhardt, I., Hwang, J., Zumofen, G. & Sandoghdar, V. Efficient coupling of photons to a single molecule and the observation of its resonance fluorescence. *Nature Phys.* **4**, 60–66 (2008).
23. Lettow, R. *et al.* Realization of two Fourier-limited solid-state single-photon sources. *Opt. Express* **15**, 15842–15847 (2007).

24. Lounis, B., Jelzko, F. & Orrit, M. Single molecules driven by strong resonant fields: hyper-Raman and subharmonic resonances. *Phys. Rev. Lett.* **78**, 3673–3676 (1997).
25. Klar, T., Jakobs, S., Dyba, M., Egner, A. & Hell, S. W. Fluorescence microscopy with diffraction resolution barrier broken by stimulated emission. *Proc. Natl Acad. Sci. USA* **97**, 8206–8210 (2000).
26. Kühn, S., Håkanson, U., Rogobete, L. & Sandoghdar, V. Enhancement of single molecule fluorescence using a gold nanoparticle as an optical nano-antenna. *Phys. Rev. Lett.* **97**, 017402 (2006).
27. Rogobete, L., Kaminski, F., Agio, M. & Sandoghdar, V. Design of nanoantennae for the enhancement of spontaneous emission. *Opt. Lett.* **32**, 1623–1625 (2007).
28. Chizhik, A. *et al.* Tuning the fluorescence emission spectra of a single molecule with a variable optical subwavelength metal microcavity. *Phys. Rev. Lett.* **102**, 073002 (2009).
29. Stobin'ska, M., Alber, G. & Leuchs, G. Perfect excitation of a matter qubit by a single photon in free space. *Europhys. Lett.* **86**, 14007 (2009).
30. Gerhardt, I. *et al.* Coherent state preparation and observation of Rabi oscillations in a single molecule. *Phys. Rev. A* **79**, 011402(R) (2009).

Acknowledgements This work was supported by the Swiss National Foundation (SNF) and ETH Zurich (QSIT, grant no. PP-01 07-02). We thank I. Gerhardt and G. Wrigge for their contributions to this project. V.S. thanks X. S. Xie for his hospitality at Harvard University during the writing process of this manuscript.

Author Information Reprints and permissions information is available at www.nature.com/reprints. Correspondence and requests for materials should be addressed to V.S. (vahid.sandoghdar@ethz.ch).